Supplementary Information

Response to solvent stimulation of terbium-organic framework for photocatalysis CO_2 reduction

Xin Lu‡[a], Zhilong Yao‡[a], Xiaomin Yuan[a], Yao Wei[a], Zhihao Zhu*[a], Hegen Zheng*[b], Chuanlei Zhang*[ab]

a. Anhui Key Laboratory of Photoelectric-Magnetic Functional Materials, Anhui Key Laboratory of Functional Coordination Compounds, School of Chemistry and Engineering, Anqing Normal University, Anqing 246011, China.

b. State Key Laboratory of Coordination Chemistry, School of Chemistry and Chemical Engineering, Collaborative Innovation Center of Advanced Microstructures, Nanjing University, Nanjing 210023, P. R. China

Tab. S1 Crystal data and structural refinements parameters of **AQNU-4**.

Complex	**AQNU-4**
Empirical formula	$C_{39}H_{57}O_{20}Tb$
Formula weight	1018.78
Crystal system	Triclinic
Space group	*P***Error!**
a / Å	9.4513(4) A
b / Å	15.2354(7)
c / Å	18.4015(8)
α / °	108.9470(10)
β/ °	95.4730(10)
γ/ °	93.3720(10)
V / Å^3	2483.35(19)
Z	2
D_{calcd} / g cm^{-3}	1.072
μ / mm^{-1}	1.465
F(000)	926
θ min-max / °	1.420, 28.392
Tot., uniq. data	18150, 12291
R(int)	0.0759
Nres, Npar	7, 436
R_1, wR_2 [$I > 2\sigma(I)$]	0.0426, 0.0843
R_1, wR_2 [*all data*]	0.0565, 0.0868
GOF on F^2	1.064
Min. and max resd dens (e·Å^{-3})	-1.027, 1.731

Tab. S2 Selected Bond Lengths (Å) and Angles (deg) for **AQNU-4**.

AQNU-4			
O(8)-Tb(1)#1	2.337(3)	Tb(1)-O(1)	2.304(3)
O(1W)-Tb(1)	2.574(3)	Tb(1)-O(2W)	2.516(3)
Tb(1)-O(2)#1	2.380(3)	Tb(1)-O(7)	2.340(2)
Tb(1)-O(4)#3	2.341(2)	Tb(1)-O(3)#2	2.321(3)
O(1)-Tb(1)-O(8)#1	73.64(10)	O(1)-Tb(1)-O(3)#2	144.11(11)
O(2W)-Tb(1)-O(1W)	126.18(10)	O(2)#1-Tb(1)-O(1W)	69.53(10)

O(7)-Tb(1)-O(1W)	138.59(11)	O(4)#3-Tb(1)-O(1W)	69.09(11)
O(3)#2-Tb(1)-O(1W)	69.82(11)	O(8)#1-Tb(1)-O(1W)	70.83(11)
O(1)-Tb(1)-O(1W)	139.30(11)	O(2)#1-Tb(1)-O(2W)	138.42(10)
O(7)-Tb(1)-O(2W)	69.95(10)	O(4)#3-Tb(1)-O(2W)	73.15(10)
O(3)#2-Tb(1)-O(2W)	72.09(11)	O(8)#1-Tb(1)-O(2W)	138.41(11)
O(1)-Tb(1)-O(2W)	72.45(11)	O(7)-Tb(1)-O(2)#1	75.78(10)
O(4)#3-Tb(1)-O(2)#1	138.42(11)	O(3)#2-Tb(1)-O(2)#1	81.46(10)
O(8)#1-Tb(1)-O(2)#1	81.30(10)	O(1)-Tb(1)-O(2)#1	123.59(9)
O(4)#3-Tb(1)-O(7)	142.97(10)	O(3)#2-Tb(1)-O(7)	83.53(9)
O(8)#1-Tb(1)-O(7)	125.64(9)	O(1)-Tb(1)-O(7)	79.39(10)
O(3)#2-Tb(1)-O(4)#3	88.16(9)	O(8)#1-Tb(1)-O(4)#3	81.68(9)
O(1)-Tb(1)-O(4)#3	86.86(10)	O(8)#1-Tb(1)-O(3)#2	140.44(11)

Symmetry Codes for **1:** #1 = – *x* + 2, – *y* + 1, – *z* + 2; #2 = *x*, *y*, *z* + 1; #3 = – *x* + 1, – *y* + 1, – *z* + 1; #4 = – *x* + 2, – *y* + 2, – *z* + 3; #5 = *x*, *y*, *z* – 1.

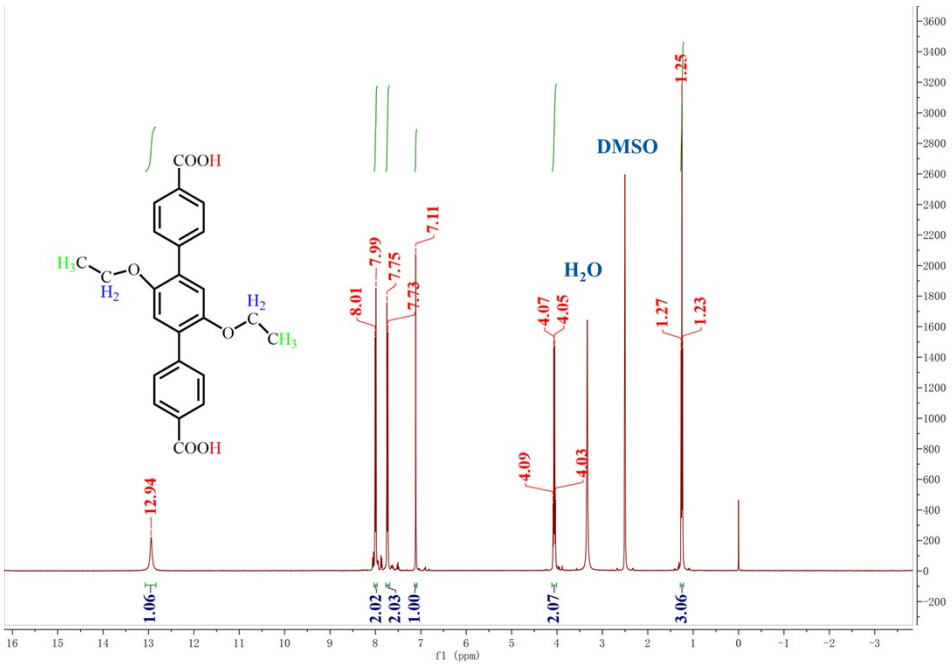

Fig. S1 ^{1}H NMR spectrum of DTDA.

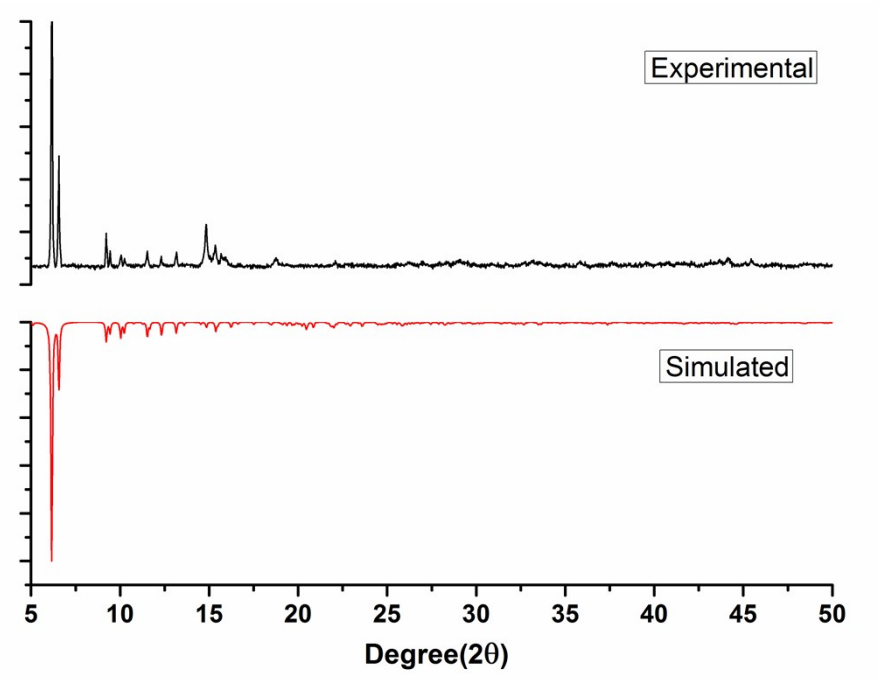

Fig. S2 Powder X-ray diffraction patterns of **AQNU-4**.

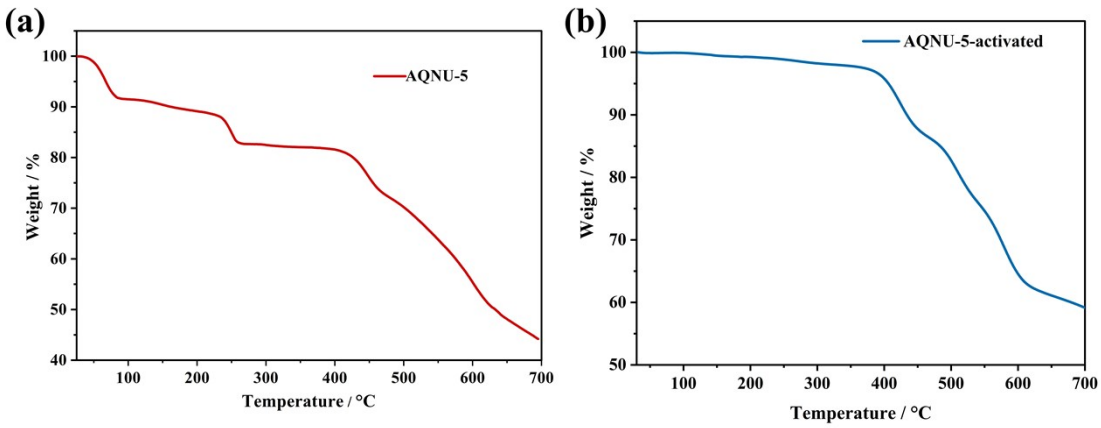

Fig. S3 Thermogravimetric curves of **AQNU-4** before and after activation.

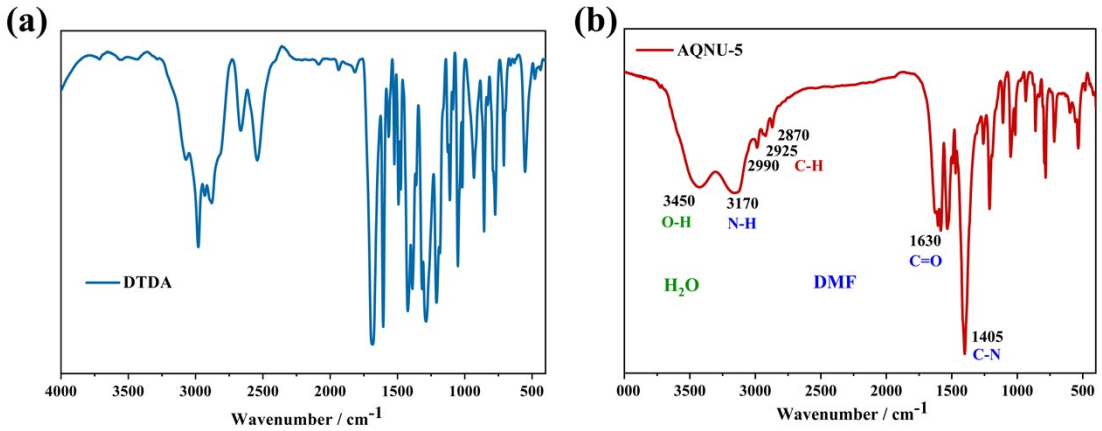

Fig. S4 Infrared spectrum of ligand DTDA (a) and **AQNU-4** (b).

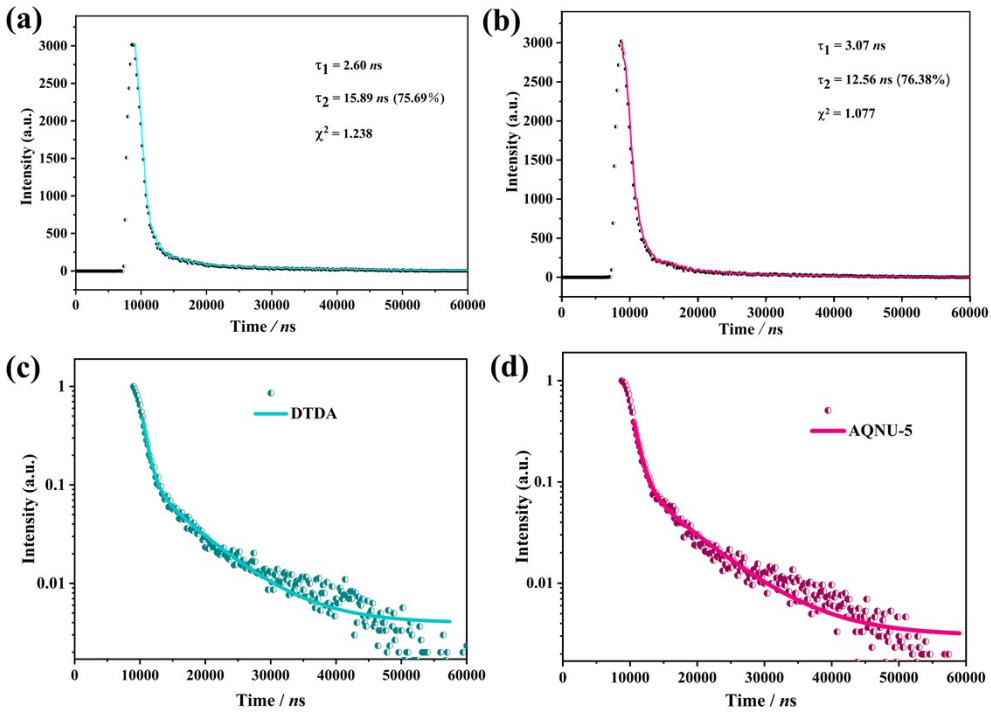

Fig. S5 The fitted decay curve in the solid state at room temperature (monitored at 452 nm for DTDA ligand, (a, c); 425 nm for **AQNU-4**, (b, d)). The sample was excited at 343 nm. Scattered line: experimental data; Solid line: fitted by Fit = $A+B_1\times\exp(-t/\tau_1)+B_2\times\exp(-t/\tau_2)$.

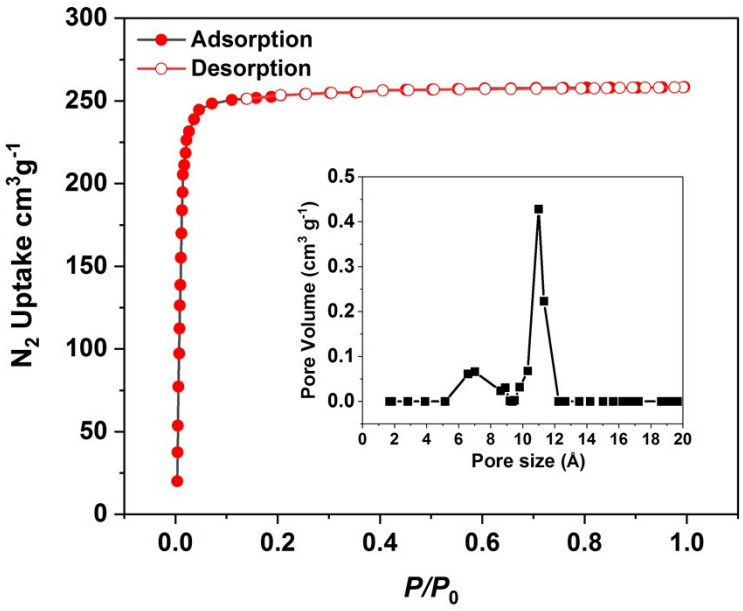

Fig. S6 N_2 sorption isotherm of **AQNU-4** at 77 K and the corresponding pore diameter distribution (inset) based on DFT model.

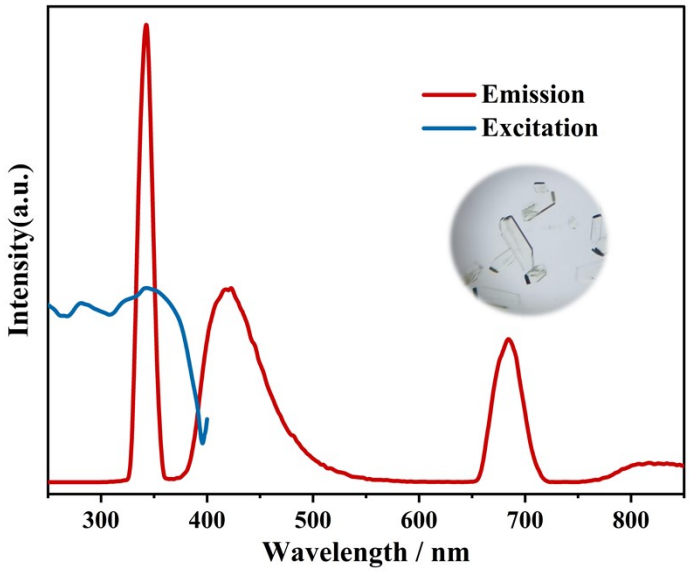

Fig. S7 Fluorescence excitation and emission spectra of **AQNU-4** (the inset picture shows a real shot).

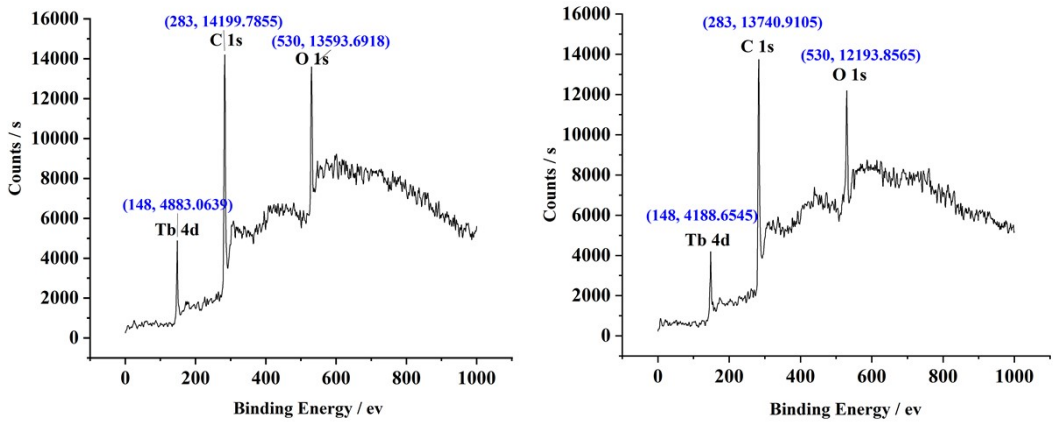

Fig. S8 Survey XPS spectra of **AQNU-4** before and after activation.

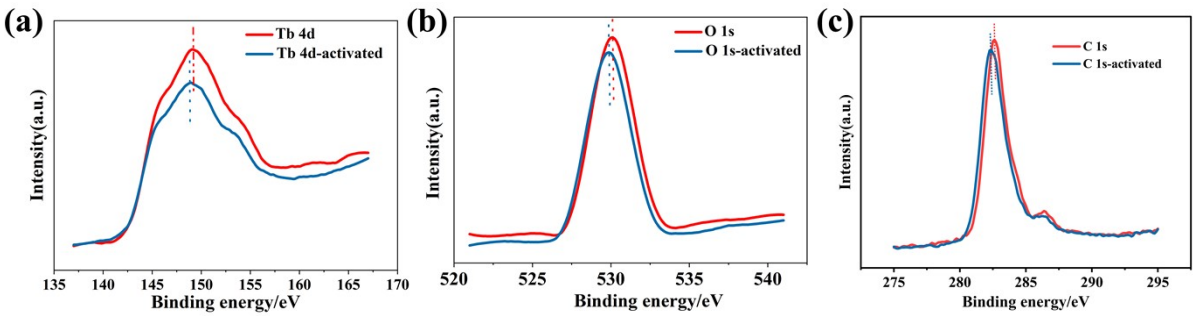

Fig. S9 The Tb 4d (a), O 1s (b) and C 1s (c) XPS spectrum before and after activation.

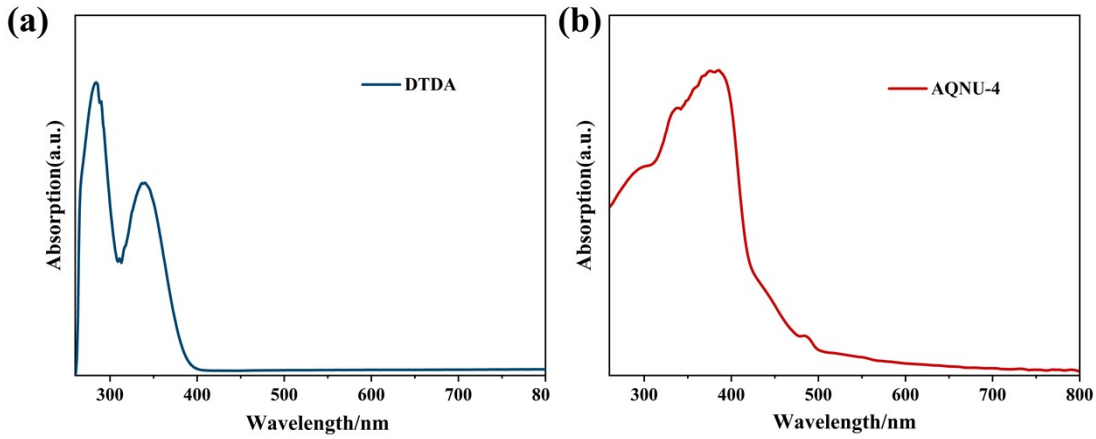

Fig. S10 The UV-Vis absorption spectra of DTDA (a) and **AQNU-4** (b).

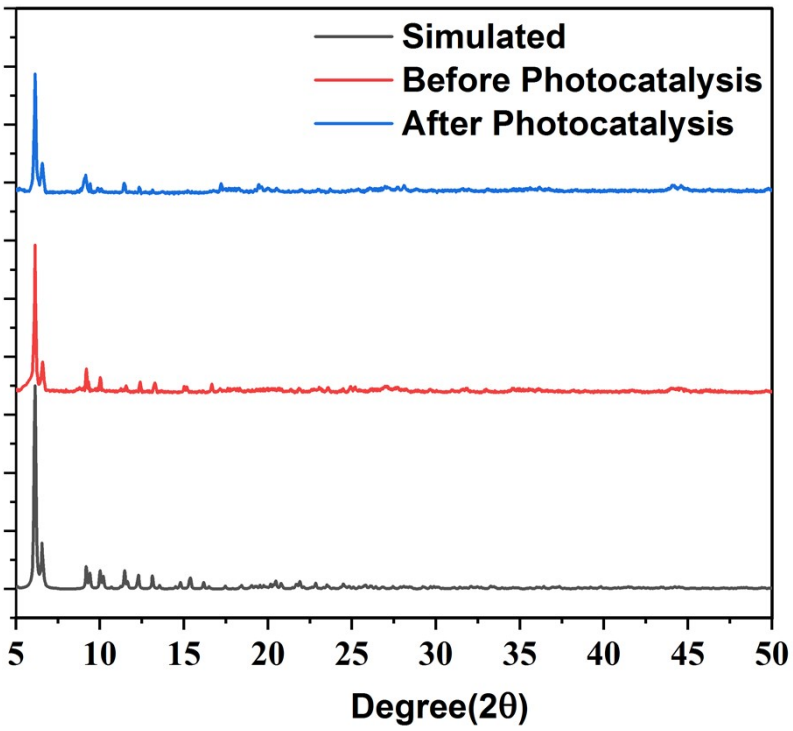

Fig. S11 PXRD of **AQNU-4** post-photocatalysis in cyclohexanone.

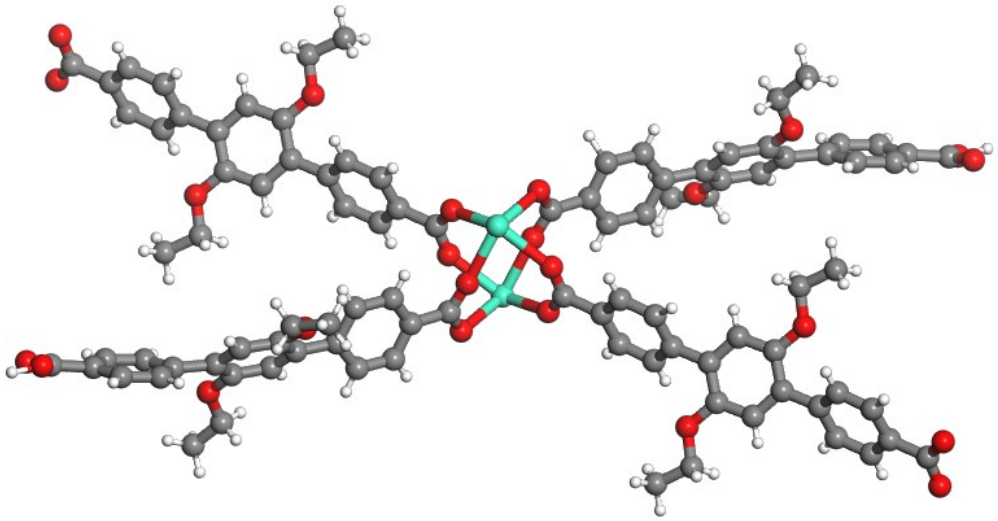

Fig. S12 The DFT computational model of structure **AQNU-4**.

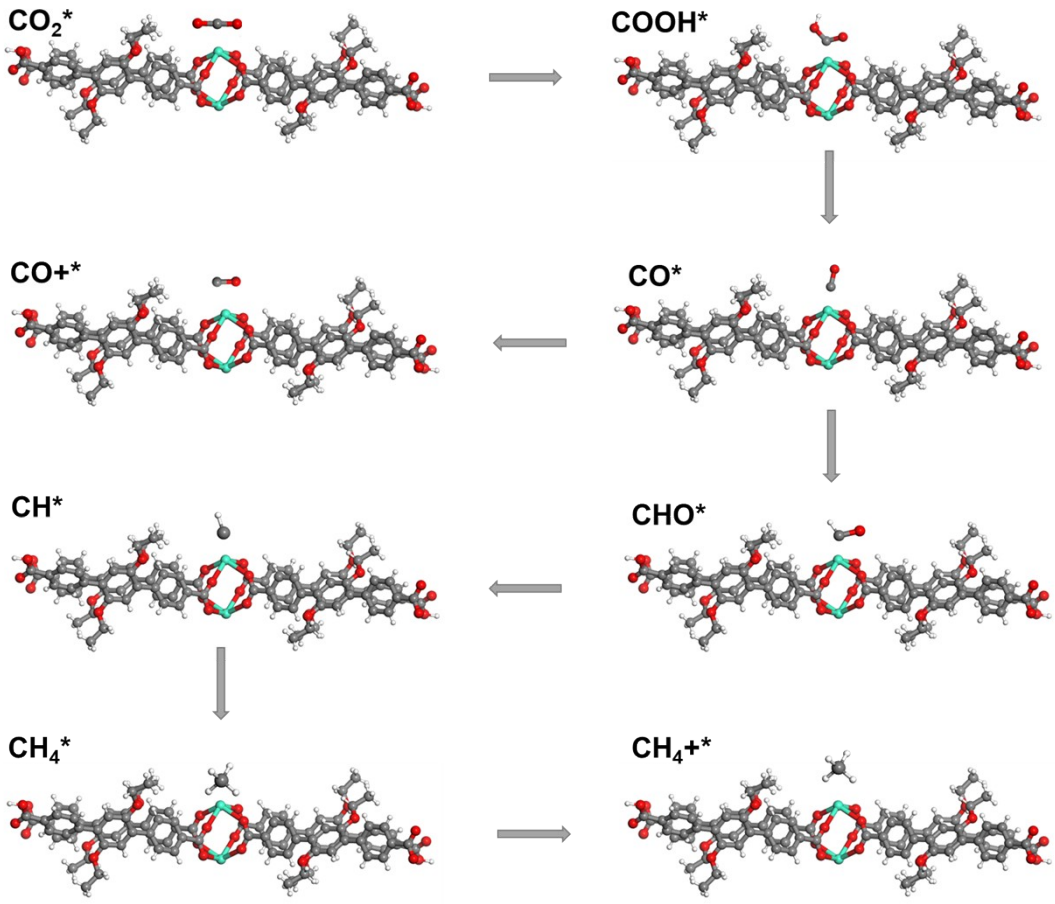

Fig. S13 Geometric configurations of **AQNU-4** in the reaction path of photocatalysis CO_2 reduction.

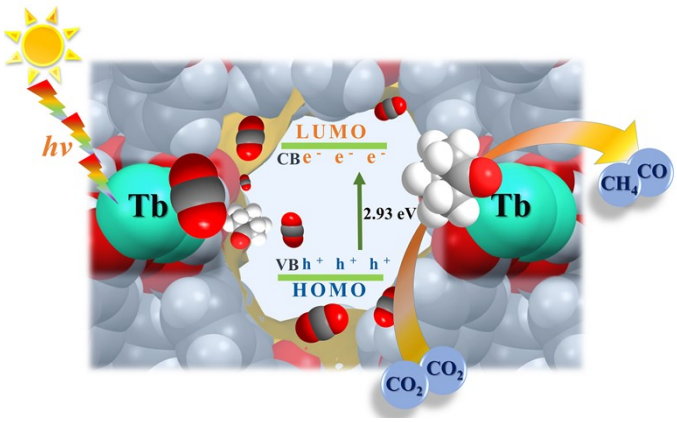

$CO_2(g) + * \longrightarrow CO_2*$

$CO_2* + H^- + e^- \longrightarrow COOH*$

$COOH* + H^- + e^- \longrightarrow CO* + H_2O(g)$

$CO* \longrightarrow CO(g) + *$

$CO* + H^- + e^- \longrightarrow CHO*$

$CHO* + H^- + e^- \longrightarrow CH* + H_2O(g)$

$CH* + H^- + e^- \longrightarrow CH_2*$

$CH_2* + H^- + e^- \longrightarrow CH_3*$

$CH_3* + H^- + e^- \longrightarrow CH_4*$

$CH_4* \longrightarrow CH_4(g) + *$

Fig. S14 The mechanistic path for CO_2 reduction reaction.